Abstracting Attribute Space for Transfer Function Exploration and Design

Ross Maciejewski, *Member*, *IEEE*, Yun Jang, Insoo Woo, Heike Jänicke, *Member*, *IEEE*, Kelly P. Gaither, *Member*, *IEEE*, and David S. Ebert, *Fellow*, *IEEE*

Abstract—Currently, user centered transfer function design begins with the user interacting with a one or two-dimensional histogram of the volumetric attribute space. The attribute space is visualized as a function of the number of voxels, allowing the user to explore the data in terms of the attribute size/magnitude. However, such visualizations provide the user with no information on the relationship between various attribute spaces (e.g., density, temperature, pressure, x, y, z) within the multivariate data. In this work, we propose a modification to the attribute space visualization in which the user is no longer presented with the magnitude of the attribute; instead, the user is presented with an information metric detailing the relationship between attributes of the multivariate volumetric data. In this way, the user can guide their exploration based on the relationship between the attribute magnitude and user selected attribute information as opposed to being constrained by only visualizing the magnitude of the attribute. We refer to this modification to the traditional histogram widget as an abstract attribute space representation. Our system utilizes common one and two-dimensional histogram widgets where the bins of the abstract attribute space now correspond to an attribute relationship in terms of the mean, standard deviation, entropy, or skewness. In this manner, we exploit the relationships and correlations present in the underlying data with respect to the dimension(s) under examination. These relationships are often times key to insight and allow us to guide attribute discovery as opposed to automatic extraction schemes which try to calculate and extract distinct attributes a priori. In this way, our system aids in the knowledge discovery of the interaction of properties within volumetric data.

Index Terms—Transfer function design, volume rendering, information theory

1 Introduction

One common method that allows scientists to visually query their volume rendered data is the interactive transfer function widget. Typically, the transfer function widgets rely on either a one-dimensional (1D) or 2D histogram frequency plot of the volumetric data (e.g., [1], [2], [3]), and it is often assumed that users will have an underlying knowledge of regions of interest within the data. By using this underlying knowledge, users will then be able to create an appropriate transfer function that maps voxel values to a given attribute structure. While scientists exploring their volumetric data do have an underlying knowledge of their data, they are often novice transfer function designers.

- *R. Maciejewski is with the Arizona State University, PO Box 878809 Tempe, AZ 85287-8809. E-mail: rmacieje@asu.edu.*
- *Y. Jang is with the Sejong University, 98 Gunja-Dong, Gwangjin-Gu, Seoul 143-747, South Korea. E-mail: jangy@sejong.edu.*
- *I. Woo and D.S. Ebert are with the School of Electrical and Computer Engineering, Purdue University, Electrical Engineering Building, 465 Northwestern Avenue, West Lafayette, Indiana 47907-2035. E-mail: iwoo@purdue.edu, ebertd@ecn.purdue.edu.*
- *H. Jänicke is with the University of Heidelberg, Im Neuenheimer Feld 368, D-69120 Heidelberg, Germany. E-mail: heike.leitte@iwr.uni-heidelberg.de.*
- *K.P. Gaither is with the Texas Advanced Computing Center, University of Texas at Austin, Research Office Complex 1.101, J.J. Pickle Research Campus, Building 196, 10100 Burnet Road (R8700), Austin, Texas 78758-4497. E-mail: kelly@tacc.utexas.edu.*

Manuscript received 14 Jan. 2011; revised 1 July 2011; accepted 29 Mar. 2012; published online 10 Apr. 2012.
Recommended for acceptance by T. Möller.
For information on obtaining reprints of this article, please send e-mail to: tvcg@computer.org, and reference IEEECS Log Number TVCG-2011-01-0012.
Digital Object Identifier no. 10.1109/TVCG.2012.105.

A typical 1D transfer function widget is shown in Fig. 1(top). This widget was presented to five novice users (but domain experts) as part of an informal user opinion survey. The users were asked to interactively select an area of interest based solely on the histogram distribution. All users selected the singular peak of the 1D histogram. However, as shown in the resultant volume rendering of Fig. 1(top), the peak in this particular histogram is actually the least interesting portion of the data. When asked to further suggest areas of interest, the users indicated that they would be unsure of where to explore next within this data. Three users selected various ranges that would be of interest to them; however, all users indicated that they were likely to start exploring such data at peak values.

In order to overcome such issues, we propose to enhance the conventional 1D and 2D histogram transfer function widgets to better capture attributes and correlations that exist in the data. To do this, we create a new mapping of the statistical properties found within the histogram bins and overlay this as a new visual representation within the traditional histogram views. Essentially, an underlying statistical property of the voxels within each histogram bin is computed with respect to a user selected attribute of interest. This statistical value is then used to guide interaction within the transfer function space, providing a visualization of the *abstracted attribute space* representation. No new attribute spaces are being created; instead, the user is presented with more information about the statistical relationships between volumetric attributes.

The same five users were presented with the new abstracted attribute space shown in Fig. 1(bottom). Again, they were asked to interactively select an area of interest. In the abstracted attribute space, the users now have a variety

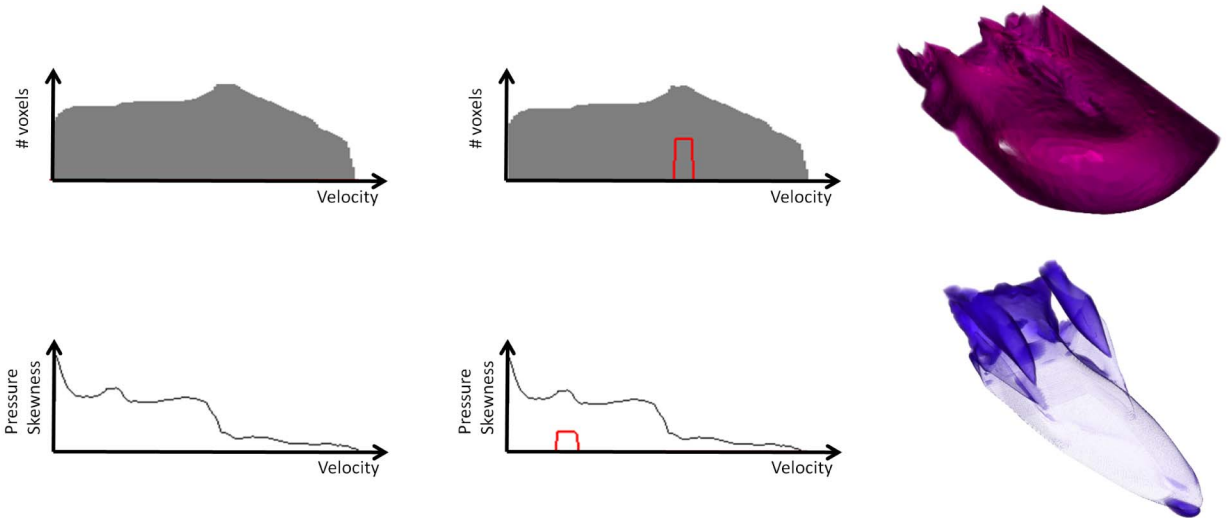

Fig. 1. Comparing explorations of the X38 experimental aircraft data using a traditional 1D histogram widget (top) and the pressure skewness abstracted 1D histogram widget (bottom). In the top image, the user is presented with only the velocity histogram. By selecting the area with the largest number of voxels, no interesting structures will be visible. By selection, we mean that the red line shown will now map opacity to the corresponding voxels. In bottom image, the user is presented with the abstracted histogram showing the skewness of the velocity histogram bins with respect to the pressure distribution in each bin. Here, the user explores the noticeable peak in the data and finds that it corresponds to the vortex cores in the data. Note that some of these regions correspond to interesting isosurface values that would be less intuitive to select when looking at the nonabstracted histogram plot. However, the same transfer function design in either widget would result in the same volume rendering.

of peaks to choose from, and many of these peaks map to interesting features of their data. Fig. 1(bottom) illustrates the resultant rendering of the most common peak chosen by the users. Other areas chosen include the leftmost area of high slope and the rightmost area of high slope.

Such an abstraction does not improve the user's ability to separate previously inseparable features. In fact, the traditional 1D histogram widget and the abstracted 1D histogram widget map the exact same voxels to the same histogram bin. Thus, if features of the volume (e.g., skin, bone) were to map to the same density bin in the original histogram, they would still map to the same bin in the abstracted space. The benefit of abstracting the histogram space is that it can provide insight to novice users with regards to the initial creation of an appropriate transfer function. Furthermore, such an abstraction is also beneficial for expert users as these statistics provide more information helping target search and analysis while exploring relationships between variables that cannot be shown with the traditional 1D histogram.

For example, extracting, representing, and understanding the properties and interactions within computational fluid dynamic (CFD) simulations has generally proven to be a difficult problem. Scientists are interested in locating critical points, vortices, shocks, and other attributes within their data and understanding the effects that various attributes (temperature, pressure, velocity, etc.) have on the volumetric flow structure. However, locating and visualizing such attributes is extremely difficult as the criteria defining flow features (e.g., shock) are often not well understood, imprecisely defined, and complex to extract volumetrically. For example, Banks and Singer [4] review eight different schemes for identifying vortices, and Ma et al. [5] listed three data properties that indicate the presence of a shock within the data. Thus, in extracting flow properties there is a need for enhanced information in understanding the interactions between the volumetric flow attribute values.

Furthermore, scientists are not only interested in the volumetric shapes and locations of the attributes, but also how these attributes interact and influence other attributes. Examples of questions that scientists may want to ask of their data are: "What effect do pressure and temperature have on velocity, and what does this correlation reveal about the physical domain?" By providing domain experts with an overlay of statistical relationships between variables in the histogram space, hypotheses can be formed and insights confirmed.

Thus, our work focuses on the mapping of statistical properties in combination with the traditional histogram widgets, thereby providing users with more information and cues on where they can begin volume exploration, as well as aiding in both transfer function design and knowledge discovery. The contribution of this work is the algorithm for generating the abstracted attribute space as well as the introduction of this space into the traditional 1D and 2D histogram widgets. By using our algorithm and modified widgets, users are able to explore the 1D abstracted transfer function space combining a variety of attributes (e.g., density, temperature, pressure, or x, y, and z dimensions simultaneously). Users can also toggle between the conventional 2D transfer function view, (in which the entries in the 2D histogram are colored by the number of voxels that map to a location) and the abstracted transfer function view, (in which the entries are colored by a derived statistical relationship). In this manner, we explore the usefulness of abstracting statistical properties in transfer function widgets and illustrate the effects on the exploration of the attribute space. We discuss the benefits and drawbacks of such an approach and illustrate our results across various volumetric data sets.

2 Related Work

Interactive transfer function design has been addressed with many different approaches, ranging from simple (yet

intuitive) 1D transfer functions (e.g., [1], [2]) in which a scalar data value is mapped to color and opacity, to more complex multidimensional transfer functions in which color and opacity are mapped across multiple variables. Early work by Kindlmann and Durkin [6] and Kniss et al. [3] applied the idea of a multidimensional transfer function [7] to volume rendering. This work identified key problems in transfer function design, noting that many interactive transfer function widgets lack the information needed to guide users to appropriate selections, making the creation of an appropriate transfer function essentially trial-and-error which is further complicated by the large degrees of freedom available in transfer function editing. While many volume rendering systems have adopted multidimensional transfer function editing tools, the creation of an appropriate transfer function is still difficult as the user must understand the dimensionalities of the attribute space that they are interacting with.

Recent work on transfer function design has proposed higher dimensional transfer functions based on mathematical properties of the volume. Examples include the Contour Spectrum by Bajaj et al. [8] which proposed a user interface for displaying computed contour attributes using the surface area, volume, and the gradient integral of the contour. Work by Kindlmann et al. [9] employed the use of curvature information to enhance multidimensional transfer functions, and Tzeng et al. [10] focused on higher dimensional transfer functions which use a voxel's scalar value, gradient magnitude, neighborhood information, and the voxel's spatial location. Work by Potts and Möller [11] suggested visualizing transfer functions on a log scale in order to better enhance attribute visibility. Lundström et al. introduced the sorted histogram [12], the partial range histogram [13], and the α-histogram [14] as means for incorporating spatial relations into the transfer function design. Correa and Ma introduced size-based transfer functions [15] which incorporate the magnitude of spatial extents of volume attributes into the color and opacity channels and visibility-based transfer functions [16] where the opacity transfer function is modified to provide better visibility of attributes. Maciejewski et al. [17] proposed a method to structure attribute space in order to guide users to regions of interest within the transfer function histogram, and Bruckner and Möller [18] depicted similarities of isosurfaces through the use of mutual information theory. While such extensions enhance the volume rendering and provide a larger separability of volumetric attributes, they still fail to provide users with information about the structures within a given attribute space. In fact, the addition of more dimensionality into the transfer function is often automatically incorporated into the rendering parameters, obscuring the relationship between the volumetric properties and the volume rendering.

Other work has focused on means of better displaying the data dimensionality to users, aiding the attribute space exploration. Shamir [19] applied attribute-space cluster analysis to unstructured meshes in order to automatically incorporate spatial information for identify structures within the volume. This clustering is performed across a 5D space (the x, y, and z components of the volume and the value versus value gradient magnitude attribute space), where as we only perform this on the attribute space. However, the goal of Shamir's work was volume segmentation as opposed to transfer function design and interactive attribute extraction. Work by Roettger et al. [20] also generated transfer functions through attribute space analysis. They enable the automatic setup of multidimensional transfer functions by adding spatial information to the histogram of the underlying data set. Work by Henze [21] developed a system in which users can interact with a variety of attribute space views, interactively brushing and linking data, thereby allowing the user to define a set of data conditions over a variety of attributes. Woodring and Shen [22] proposed a method in which the user is presented with several different volumetric renderings and is able to compare values from these data sets over space and time, and combine various rendering attributes into one volumetric rendering. Akiba et al. [23], [24] utilized parallel coordinate plots to create a volume rendering interface for exploring multivariate time-varying data sets. By means of a prediction-correction process, Muelder and Ma [25] proposed to predict the attribute regions in the previous frame, making the attribute tracking coherent and easy to extract the actual attribute of interest.

In all of this related work, one can note that various statistical properties of the volumes are being used in order to extract attributes of interest and segment properties of the volume. Unfortunately, as the number of dimensions increases, interaction in n-dimensional space becomes cumbersome to the point that few systems exceed 2D transfer functions; instead, the extra dimensionality is incorporated automatically, somewhat limiting the user's control. In order to enhance the information provided in the transfer function histogram widget, our work focuses on incorporating statistical properties of user selected attributes into the projected attribute space domain. Recent work on incorporating statistical and information metrics into time-varying volumetric data includes work by Fang et al. [26] on the time activity curve, Jänicke et al. on local statistical complexity analysis [27], and Haidacher et al. [28] on utilizing information theory for fusing traditional transfer function space with information enhanced transfer function spaces.

In exploring volumetric attribute space, one can think of the 2D histogram widget as a special form of a scatterplot where the points are binned as opposed to plotted individually. Scatterplots have long been recognized as a useful tool for multidimensional visualization due to their relative simplicity and high visual clarity [29], [30], and have been incorporated in a number of multidimensional visualization toolkits (e.g., Tableau/Polaris [31], GGobi [32], XmdvTool [33]). While recent work explored methods to enhance user interactions across the entire attribute space of a multidimensional data set using scatterplot matrices [34], little work has been done in regards to incorporating attribute relationship visualizations into scatterplots. Some work in that area includes methods by Wang et al. [35] that introduces an importance-driven time-varying data approach, work in brushing moments by Kehrer et al. [36], and the statistical transfer-function space work by Haidacher et al. [37]. In Wang et al. [35], a user is presented with importance curves based on the temporal component of the data. Other work on analyzing statistical properties within

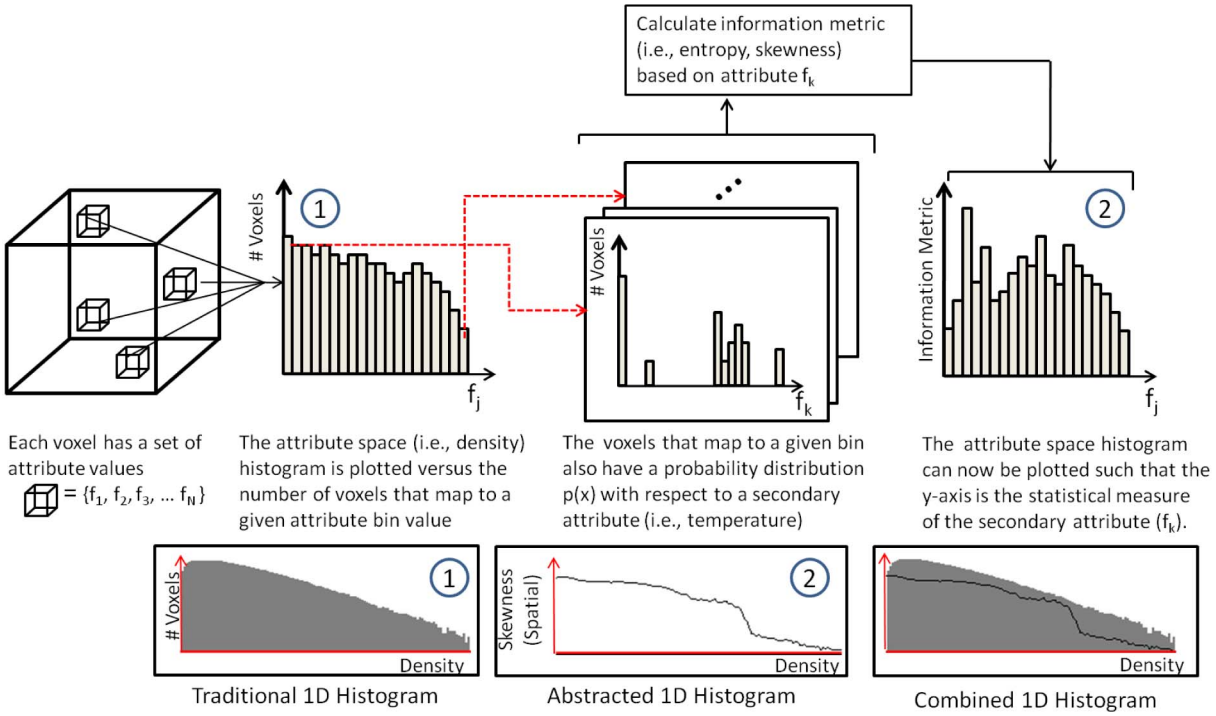

Fig. 2. The attribute space abstraction pipeline for the 1D histogram case. The algorithm is the same for the 2D histogram case.

transfer function space includes the work by Bachthaler and Weiskopf. Their work includes a method to create a continuous scatterplot [38] relating traditional discrete histograms to the histograms of isosurface statistics and they extend this work [39] to utilize subdivision within the spatial domain for creating continuous scatterplots and show their applications in volumetric rendering. In Kehrer et al. [36] the authors estimate statistical moments of the data including the mean, standard deviation, skewness, and kurtosis and apply this to the analysis of multivariate scientific data. In Haidacher et al. [37] the authors adaptively estimate statistical properties including the mean and standard deviation of the data values within a given neighborhood. The authors perform similarity tests within regions to determine if a material within a neighborhood is homogenous and create a new statistical transfer function space. Our work is similar to previous work where the user is presented with a variety of information metrics based on user defined specifications; however, work by Haidacher et al. creates a new transfer function space to enable the distinction of new materials. Our method does not enable the distinction of new materials. Instead, our method overlays the relationship of the current attribute being visualized in the histogram with another user selected attribute, thus providing fundamentally different views and functionality to the user.

3 Abstract Attribute Space Generation

Current transfer function design widgets typically present users with a low-dimensional projection of the volumetric attribute space onto an interactive one or 2D histogram widget. These projections represent the magnitude of a given attribute (i.e., the number of voxels that map to a given attribute). Attribute selection is then accomplished through traditional brushing of the histogram, and the voxels that map to a given attribute are assigned a color and opacity by the user.

In this work, we propose a modification to the traditional histogram transfer function design widgets. Instead of visualizing the attribute space as a function of the magnitude of the number of voxels, our work utilizes a novel pipeline that presents users with information metrics about a given attribute set. We refer to this information enhanced attribute space as an *abstract attribute space*. In our transfer function widget, a user is presented with information about the interactions between attributes within their data set as opposed to the magnitude of the volumetric attributes. Previous work has shown that there are links between the geometric properties of isosurfaces and the statistical properties of data [40], [41], and our information enhanced transfer function widgets help aid scientists in understanding these (and other) links. These tools aid the users by promoting new insights into volumetric data and enhance the knowledge discovery process.

Fig. 2 illustrates our abstraction pipeline in the 1D histogram attribute space case (note that the 2D abstraction process is exactly the same). Beginning with the volumetric data, each voxel consists of a set of N measured or derived attributes, $\{f_1, \ldots, f_N\}$. The user chooses any one of these volumetric attributes, $\{f_j\}$ in Fig. 2 (for example, f_j could be density), and a histogram distribution of this attribute is created. This histogram is typically found in the 1D transfer function editor widget common in many volume rendering systems.

We modify the histogram by taking the voxels that map to a given bin in the $\{f_j\}$ attribute space histogram and derive an information metric about that attribute space with respect to one or more of the remaining attributes in the

attribute space set, $\{f_k\}$ (for example, f_k could be temperature). Since the voxels corresponding to each bin in the $\{f_j\}$ histogram are known, we are able to map these voxels to a 1D distribution with respect to the user defined attribute of interest, f_k. This mapping is never shown to the user; instead, it is used to derive a set of information metrics, this information metric can then be presented to the user as a 1D plot, as shown in Fig. 2. Thus, the user is presented not with the magnitude of an attribute, but with a derived set of information about the attribute with respect to a secondary volumetric feature.

We have also extended our process to the 2D histogram widget as well. In the case of the 2D widget, the traditional 2D transfer function editor widget utilizes two attributes of the volume data $\{f_i, f_j\}$. The original histogram is plotted such that each bin is colored based on the number of voxels in each bin. The application of our algorithm will utilize a third attribute of the volume data $\{f_k\}$ and calculate the statistical properties of this feature for all voxels found in a given bin in the 2D histogram. The original histogram is then redrawn, where the color is now mapped to the derived statistical property. Examples of both the 1D and 2D abstract attribute space generation are shown throughout this paper.

In this work, we survey the use of four information metrics: mean, standard deviation, skewness, and entropy. This section details the information metric computations used, thereby formalizing the final (calculate information metric) step in our abstraction pipeline (Fig. 2). This final step in our pipeline is extensible, and future work will explore the use of other information metrics for transfer function design.

All information metrics are calculated as a precomputation step during volume loading and the resulting attribute space plots can be toggled between in real time. Precomputation time for a $512 \times 256 \times 128$ floating point data set takes approximately 9,093 ms for the combined 2D skewness calculations, 513 ms for the combined 2D entropy calculations, 97 ms for the combined 1D skewness calculations, and 20 ms for the combined 1D entropy calculations. Note that the mean and standard deviation calculations are incorporated as part of the skewness calculation. Results are from a $256 \times 256 \times 256$ data set on an Intel Xeon(R) CPU E5335 2.00 Ghz machine with 4 GB of RAM. Timings scale linearly with respect to the number of voxels.

3.1 Mean

Given an entry m in the attribute space $\{f_j\}$, we define $S_V = \{V_1, \ldots, V_Z\}$ to be the set of voxels that map to this given volume attribute. There are Z voxels that will map to this space. Within S_V, we calculate the mean, $\mu(S_V)$, with respect to the user chosen secondary attribute $\{f_k\}$

$$\mu(S_V) = \frac{1}{|S_V|} \sum_{x \in S_V} f_k(x). \tag{1}$$

The calculated mean thus depicts the average value of the f_k attribute with respect to a value range for f_j. Furthermore, this mapping provides users with more information about their data by showing them how a certain value of attribute f_j is related to values in f_k.

3.2 Standard Deviation

Once the mean is calculated, we can then determine the standard deviation, $\sigma(S_V)$, with respect to the secondary attribute $\{f_k\}$.

$$\sigma(S_V) = \sqrt{\left(\frac{1}{|S_V|} \sum_{x \in S_V} \left(f_k(x) - \mu(S_V)\right)^2\right)}. \tag{2}$$

The standard deviation of the set, S_V with respect to the f_k attribute of the voxels is then mapped back to the corresponding bin in the $\{f_j\}$ histogram attribute space.

The standard deviation thus depicts the variance of the f_k attribute values corresponding to a particular value of f_j. Areas of low standard deviation typically indicate a high correlation between the bin range of f_j and the average value of f_k found with respect to that bin. Such information can reveal relationships between data. For example, a scientist may wish to explore temperature ranges of their data in which the pressure is highly fluctuating. To do this, they would interactively select the temperature ranges where the standard deviation of the pressure is found to be large. By using this attribute mapping, such ranges can be immediately found, whereas in the traditional 1D histogram users would only be unable to see such relationships.

3.3 Skewness

Skewness is a measure of the asymmetry of the distribution of the underlying data. The skewness of a random variable is the third standardized moment about the mean and standard deviation of an underlying data distribution. Given the set of voxels S_V that map to the attribute space $\{f_j\}$ at m in the attribute space histogram, the skewness, $\gamma(S_V)$, of the voxels at that location with respect to an attribute $\{f_k\}$ (e.g., velocity, enstrophy) is calculated.

$$\gamma(S_V) = \frac{\frac{1}{|S_V|} \sum_{x \in S_V} \left(f_k(x) - \mu(S_V)\right)^3}{\left(\frac{1}{|S_V|} \sum_{x \in S_V} \left(f_k(x) - \mu(S_V)\right)^2\right)^{\frac{3}{2}}}. \tag{3}$$

Our choice of utilizing skewness as an attribute space abstraction metric is influenced by the work of Patel et al. [42] in which the authors demonstrate the effectiveness of using high order statistical moments for transfer function generation. Skewness may be either positive or negative. In the 1D transfer function case, we add a secondary axis to the plots to show positive and negative skewness. In the 2D transfer function case, we utilize a blue to red color map with blue values representing negative skewness and red being positive. Areas with high skewness typically represent inhomogeneity in the data, while areas of low skewness typically represent regions where the data are normally distributed implying some underlying structural homogeneity.

3.4 Entropy

For the entropy calculation, given the set of voxels S_V that map to the attribute space $\{f_j\}$ at m in the attribute space histogram, the entropy, $H(S_V)$, of the voxels at that location with respect to a user chosen secondary attribute $\{f_k\}$ can also be calculated

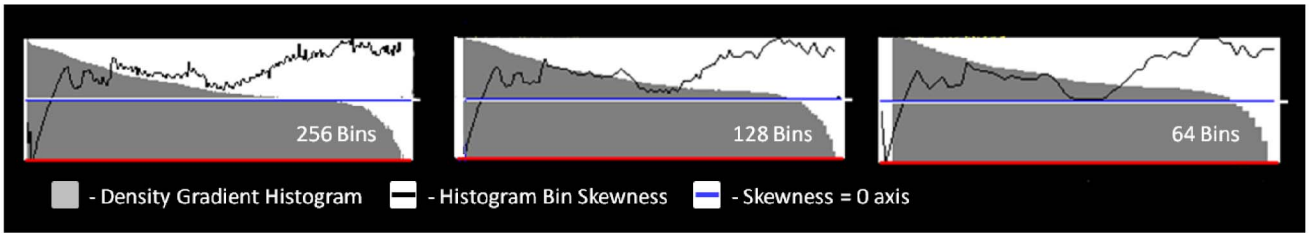

Fig. 3. Exploring the effect of the histogram bin size on abstracted attribute spaces. Here, we show the 1D density gradient histogram of the Bonsai CT data (in gray) and the skewness of the data (as a black line). As the number of bins increases, the statistical measures are smoothed.

$$H(S_V) = -\sum_{x \in S_V} p(f_k(x)) \ln(p(f_k(x))). \quad (4)$$

Here, $p(f_k(x))$ is the probability that a voxel in the set S_V has a value $f_k = x$. Since S_V is known, we can simply use the one-dimensional histogram of these voxels with respect to their f_k attribute values to calculate the probability distribution. For example, if three voxels within S_V map to $f_k = q$, then $p(f_k = q) = 3/Z$ where Z is the total number of voxels in S_V. Once $H_S(*)$ is calculated, the entropy value is mapped back to the $\{f_j\}$ histogram attribute space. The entropy depicted at each position in the abstract attribute space provides information about the extent of the corresponding set of voxels.

With regards to spatial attributes (x, y, and z), spatially isolated structures often define an attribute and low spatial entropy is well suited to indicate them. High entropy, on the other hand, is reached with a uniform distribution of voxels over the physical domain. In this case, the combination of values is likely to belong to background dynamics and corresponding positions are often irrelevant for the user.

3.5 Histogram Binning Effects

In creating the abstracted attribute space, the results are directly related to the voxels that map to a given histogram bin. Thus, the bin size (or number of bins used) will directly impact the resultant abstracted attribute space visualization. In order to understand and explore the impact that histogram binning will have on our proposed method, we have modified the number of bins used and compared the resultant abstracted attribute space plots, as shown in Fig. 3. As the number of bins decreases, the overall shape of the skewness curve remains intact; however, minor peaks are smoothed out and the bin skewness values change.

We have further explored the effects of bin sizes over all data sets presented in this paper. The shape of all abstracted attribute space curves remains consistent for all statistical measures used in our work (i.e., mean, standard deviation, entropy, and skewness). Overall, the changes to the abstracted attribute space curves seem to be minimal; however, we plan to explore adaptive histogram binning as a means of potentially extracting stronger statistical correlations.

As with all histograms, there is no such thing as a "best number" for bin size. Different choices in bin width can reveal different features about the data; however, the size of the bin will directly impact our underlying statistical measures. As the bin width gets smaller, the number of voxels that maps to each bin becomes sparser. Such sparsity can bias the data resulting in details that may appear to be random noise. Conversely, as the bins become larger, more data are being placed into each bin. In this manner, more voxels are being grouped together, and features within the volume will be less separable. Thus, it is important to choose a reasonable bin width when employing the use of our abstracted feature space metrics. Preliminary work indicates that using equal interval bins, where the number of bins is approximately the square root of the number of voxels in the volume is a reasonable approach.

4 Attribute Space Exploration Tools

In order to better facilitate volume exploration through transfer function design, we have developed a small suite of attribute space exploration tools to complement the traditional interactive transfer function design metaphors. Our tools include an expanded 1D histogram view, linked 1D and 2D histogram views for explorations into manual attribute segmentation, and an opacity brushing tool for highlighting complex attribute space structures such as arcs.

4.1 Expanded 1D Histogram View

The traditional 1D histogram view consists of the frequency space of the voxel data with a particular volumetric attribute (value, value gradient magnitude, etc.) being assigned to the x-axis of the histogram and the number of voxels this attribute maps to is assigned to the y-axis. Our expanded 1D histogram view utilizes this convention and plots the frequency distribution of both the value and value gradient magnitude space in a 1D histogram widget tool. This frequency plot is the gray background plot seen in the histograms of Fig. 4(left). Note that the left set of histograms show the value versus frequency and the right set of histograms show the value gradient magnitude versus frequency. From top to bottom, the histograms are then overlaid with a statistical plot representing some spatial information (in this case the standard deviation) of the voxels with respect to their x, y, and z positions. User interaction in any of the three windows will modify the same transfer function applied to either the value or value gradient magnitude attribute space. However, only one transfer function (the value attribute space transfer function or the value gradient attribute space transfer function) is applied for volume rendering based on the most recently edited transfer function.

4.2 Linked 1D-2D Exploration View

While the user may create a 1D transfer function, work has shown that by increasing the dimensionality of the attribute space under exploration, the separability of more attributes

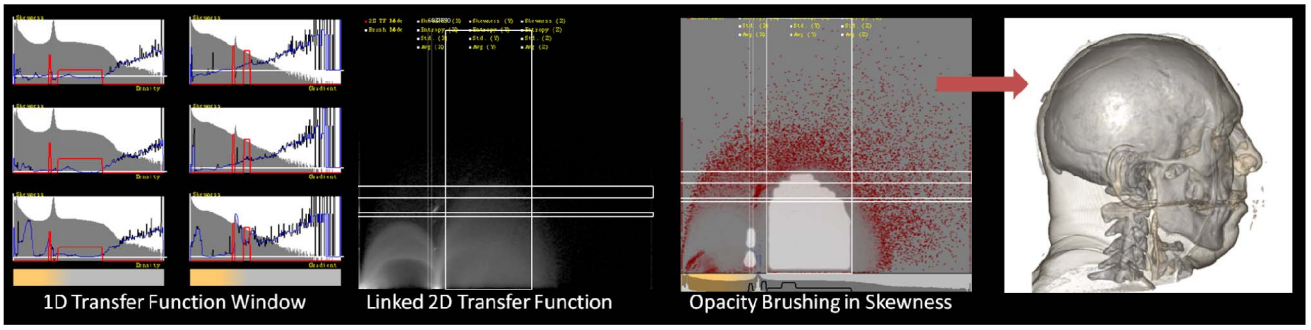

Fig. 4. Attribute space explorations tools. (Left) A hexa-window 1D histogram view showing the user the standard deviation spatial properties of the Visible Male Head data set for the x, y, and z directional data (the top, middle, and bottom views, respectively) in the density (left) and density gradient magnitude (right) attribute space. The gray area is the frequency distribution of the data. The black line is the abstracted attribute space property. The red line is the user defined transfer function representing the opacity. (Middle-Left) A 2D histogram view of the density versus density gradient magnitude histogram view with linked regions brushed based on the user defined 1D transfer function widget. (Middle-Right) A user defined transfer function in the 2D histogram view where opacity brushing was applied to explore the linked region. (Right) The resultant volume rendering from the opacity brushed transfer function. Note that the 1D transfer function was designed with respect to the z-directional skewness.

becomes possible (although this is highly influenced by the choice of dimensions). As the user modifies the transfer function space in the 1D histogram views, a linked 2D histogram view is created in which the corresponding bins are highlighted by rectangular bounding boxes so that the user may explore further details within the 2D attribute space. This linked view is shown in Fig. 4(Middle-Left). Here, the white rectangular regions depict the areas of nonzero opacity brushed by the user in the 1D histogram space.

4.3 Opacity Paintbrushing

Finally, to enhance user interaction, we utilize an opacity paintbrush tool for the 2D histogram widget similar to the painting tool described in Co et al. [43]. Traditional transfer function design widgets for 2D histograms include drawing a series of rectangular boxes and defining a color and opacity within the selected region. However, most structures that appear in the 2D attribute space are unable to easily fit within a rectangular widget. To overcome this, we utilize an opacity brushing tool in which the user has applied some underlying color map to the data, either automatically as done by Maciejewski et al. [17] or manually through rectangular widget creation or through the linked coloring from the 1D transfer function design. Fig. 4(Middle-Right) demonstrates a user created transfer function through the use of our opacity brushing widget. The application of this transfer function for volume rendering is seen in Fig. 4(Right).

4.4 Scaling by View Direction

In multivariate volumetric data, there are many attributes that can be utilized in the attribute abstraction process. In computational fluid dynamic simulations, users may have variables such as spatial position, temperature, pressure, vorticity, etc. However, in CT data, the attributes are often limited to only the density and the spatial position. While each coordinate of the spatial attribute could be mapped to its own separate value, this then requires the user to mentally integrate the three vector components. To handle this case, our system provides the users with two options: each component of the spatial attribute (x, y, and z) are plotted in a separate graph and presented to the user (as shown in Fig. 4), or the view direction is used to scale the information vector and the scaled value is shown to the user (Fig. 5). The scaling of the spatial attribute vector based on the view direction is defined as follows:

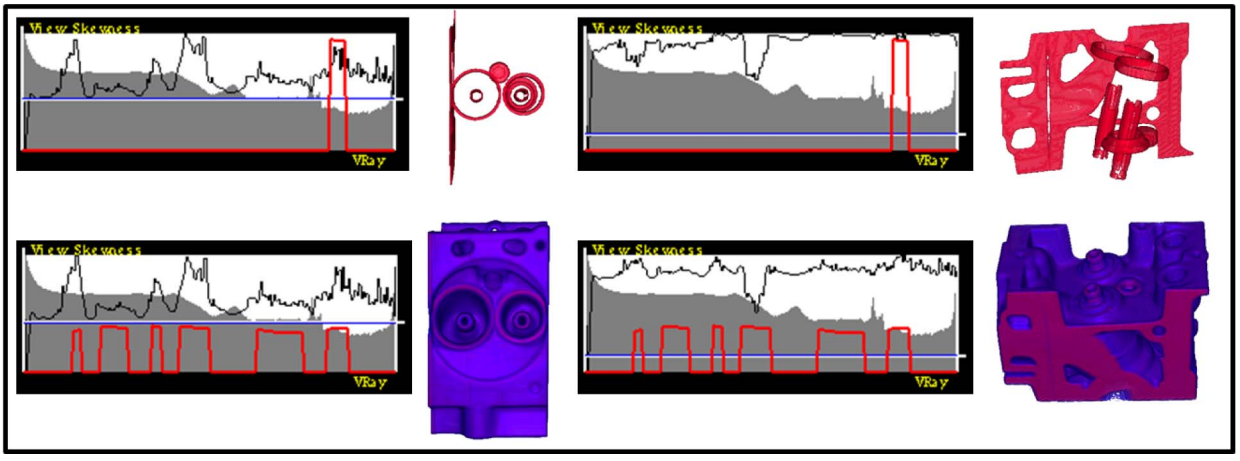

Fig. 5. Exploring CT data using abstracted attribute spaces. The histogram shows the 1D density attribute space of the Engine data. Here, the user has selected various regions of high skewness for analysis and explores the effect the view direction has on the data skewness. Note that the underlying histogram distribution is the same in both the right and left image transfer functions; however, the overlaid skewness plot varies based on the viewing angle. The red line in the histogram widget is the user defined opacity.

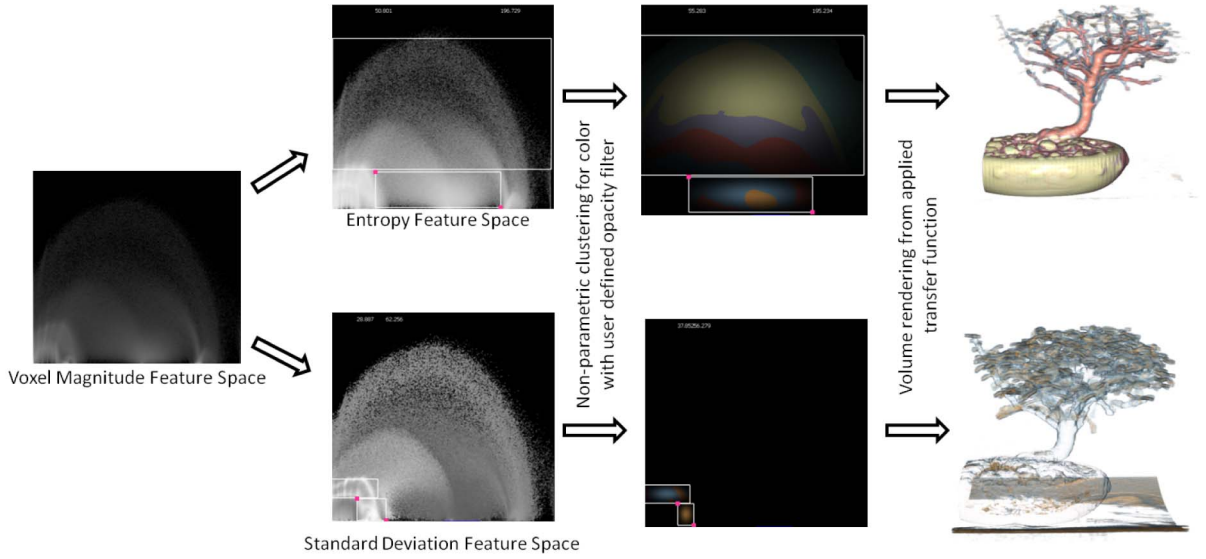

Fig. 6. Exploring CT data using abstracted attribute spaces. The density versus density gradient magnitude attribute space of the Bonsai data.

$$S = \frac{A_x V_x + A_y V_y + A_z V_z}{\sqrt{A_x^2 V_x^2 + A_y^2 V_y^2 + A_z^2 V_z^2}}, \quad (5)$$

where A_x, A_y, and A_z are the information metrics calculated with respect to the spatial attributes (x, y, and z), and V is defined as the view directional vector calculated as

$$V = M^{-1}[0\ 0\ -1]^T, \quad (6)$$

where M is the camera matrix.

We illustrate the effect that scaling by view direction has on the data exploration process in Fig. 5. Here, we explore skewness as an information metric in CT data utilizing the x, y, and z components of the voxels in the volumetric space and calculate the skewness with respect to each direction for each bin in the 1D histogram. The spatial skewness is then scaled and normalized based on the view directional vector of the volume and plotted as a black line on top of the density histogram plot. In the density 1D attribute space (Fig. 5(top)), we can see that the skewness provides new peaks in the data to explore that are not evident in the traditional frequency plot (the underlying gray histogram).

In Fig. 5(Top-Left) the user explores a peak of particular interest in the upper range of the density values. As the viewpoint changes, the user defined transfer function remains constant; however, the spatial skewness changes as is seen in Fig. 5(Top-Right). Using the same view point in Fig. 5(Bottom-Left), we highlight all the skewness plateaus and explore the resulting visualization. Again, we see that changing the viewpoint results in a change in the plotted spatial skewness Fig. 5(Bottom-Right).

Here, the user has interactively selected various areas in the plots based on either high skewness peaks or rates of change in the skewness. This process is similar to that shown in Fig. 1 where the user explores various peaks in the abstracted space. Our final rendering shows only a subset of the peaks after exploration was done. From this we can see that the information metric provides new cues as to which regions in a data set may be of interest for visualizing results. Depending on the data alignment, different information about material boundaries and segmentation regions can be found. Future work will look at incorporating these various information metrics as a means of shading parameters.

5 Attribute Space Exploration Examples

In this section, we survey the meaning of our abstract attribute space representations in the context of the related volumetric properties. First, we illustrate the effect of using the abstract attribute space in a traditional CT data set in order to illustrate the meaning of the attribute space entropy. Second, we present a case study exploration of CFD data using the derived abstract attribute space representations. Finally, we explore the effect of noisy data on our derived abstract attribute space representations.

5.1 Spatial Abstract Attribute Spaces

5.1.1 Entropy and Standard Deviation

A key step in utilizing the abstract attribute space representation effectively for volume exploration is understanding the notion of entropy. As stated in Section 3.3, locations in the attribute space that consist of high spatial entropy are unlikely to represent structures within the data. In Fig. 6(Top), the user is comparing the traditional voxel magnitude-based attribute space representation to the entropy-based representation. Here, we can quickly see that the area of the highest entropy maps to that of the highest number of voxels. As this is likely the air surrounding the volumetric data, the user chooses to segment the data by utilizing a square opacity filter in the entropy attribute space. The underlying colors are based on the nonparametric transfer function generation of Maciejewski et al. [17]. Here, we see that the most spatially coherent volumetric structures are able to be quickly extracted from the data.

Given the spatial randomness of the leaves, it is likely that the spatial standard deviation will be able to guide the user in segmenting the leaves. In Fig. 6(bottom), the user switches to the spatial standard deviation attribute space. In the lower right corner, a particularly high band of standard

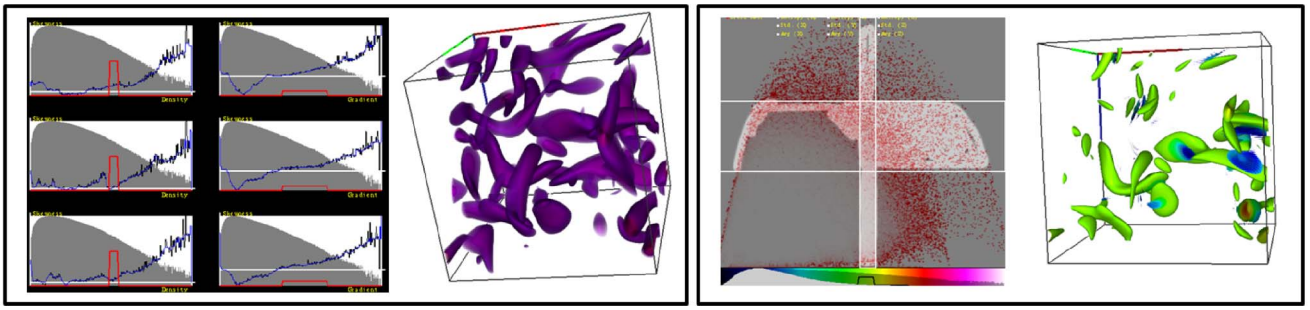

Fig. 7. Exploring the turbulent vortex data using skewness. (Left) The value attribute space of the vortex data where the user has extracted areas of low skewness in the z spatial direction and the resultant rendering. (Right) The value versus value gradient magnitude attribute space where the user has selected regions of high skewness within the previously selected 1D transfer function regions and the resultant rendering. The red line in each 1D histogram widget represents the user defined opacity.

deviation is evident to the user. Again, using a combination of square opacity filters, the user is able to directly segment the leaves. As such, one can see that by using a combination of abstract attribute space representations, a user is able to quickly and effectively explore their volumetric data.

While the use of abstract attribute spaces does allow the user to find very clean segmentation areas within the volume, in CT and MRI data, there are known properties of the density versus density gradient attribute space that allow users to create transfer functions by selecting the arc like structures within the attribute space. These arc-like structures correspond to material boundaries, and these cues have been shown to aid users in attribute extraction. However, CFD data do not have well-defined boundaries, and such methods are unable to extract structures such as shocks and vortices. Furthermore, when looking at an arbitrary attribute space, such as Pressure versus Velocity Magnitude, the relationships between data values may not be apparent.

5.1.2 Skewness

Fig. 7 illustrates the application of our abstract attribute space representation when applied to the turbulent vortex data set. The data set is sized at $128 \times 128 \times 128$ and is a fluid flow simulation that has been used in many studies [25], [44], [45]. Here, we explore regions of near zero skewness in the value gradient magnitude attribute space of the data and the area of high skewness change in the value magnitude attribute space with respect to the y-directional component, see the transfer function designs in Fig. 7(left). Next, we change to the 2D attribute space of value versus value gradient magnitude and highlight the regions of high skewness within the bins chosen from the 1D attribute space interactions, Fig. 7(right). This method allows us to further refine the visualization that is of particular importance with turbulent flow simulations. Areas in turbulent flow where there is a high skew level represent potential attribute areas and should be more closely explored. This high skew level highlights change in the flow. Since turbulent flow attributes can be difficult or impossible to analytically describe, highlighting regions in the flow that have attributes of interest is a powerful tool for gaining insight to these data sets.

5.2 Nonspatial Abstract Attribute Spaces

5.2.1 Skewness

As previously stated, it is often that CFD data does not have well defined boundaries. Furthermore, scientists are often interested in relationships between not only position, but also measured properties, such as temperature and velocity. Fig. 8 demonstrates the abstraction of the attribute space with respect to nonspatial properties. In Fig. 8(top), the user is exploring the relationship between the velocity and the

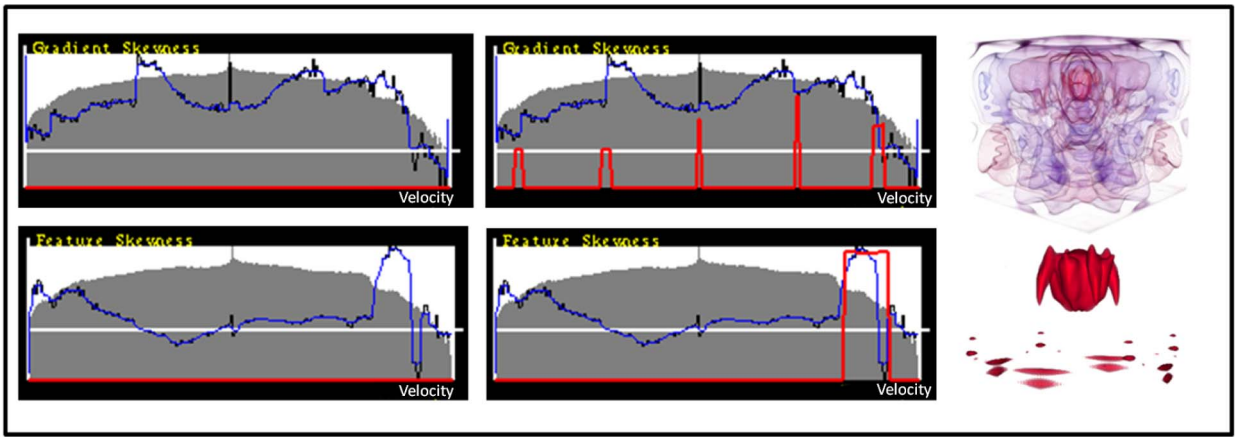

Fig. 8. Exploring the convection in a box data set with respect to nonspatial attributes (Time stamp 120). (Top) The velocity histogram overlaid with the velocity gradient skewness abstracted attribute space. (Bottom) The velocity histogram overlaid with the user defined attribute skewness (in this case the user is exploring the temperature when compared to the velocity). The red line in each 1D histogram widget is the user defined opacity.

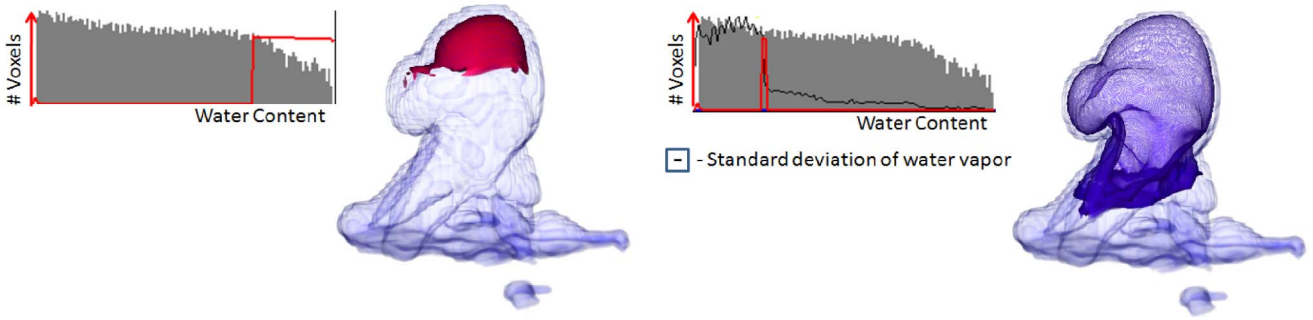

Fig. 9. Exploring the formation of a cumulus cloud with respect to the water content and water vapor values. The red line in each 1D histogram widget is the user defined opacity.

velocity gradient skewness. We create an oscillating transfer function, the peaks of which map to the skewness peaks in the gradient, creating an advection rendering similar to work by Svakhine et al. [46].

In Fig. 8(bottom), the user is exploring the relationship between the velocity and the temperature skewness. Here, the user has selected regions of highly variable temperature (both the highest and lowest range of skewness). The blue line in the bottom part of Fig. 8 is the skewness of temperature with respect to velocity. At high velocities, we can see that the temperature is nonconstant. Visualizing these values in abstract attribute space allows us to highlight areas of mixing. When discussing these plots with a domain scientist, they were able to point out that convective heat transfer takes place through both diffusion and advection, each of which can be highlighted in the abstract attribute space. The domain expert indicated that such plots were useful to her in exploring the data as it provided her with details about the underlying data relations as opposed to only a singular value distribution. In this case, the domain expert was a transfer function design expert as well. While the expert had certain value ranges in mind to explore as part of the transfer function design phase, the expert indicated that the enhanced information view presented was valuable for explaining phenomenon within the data. Furthermore, the expert indicated that such plots would be useful for detecting anomalies within simulations.

5.2.2 Standard Deviation

Our next data exploration example utilizes a cumulus cloud simulation. In Fig. 9, the user is presented with a histogram of the water content of the cloud. A conventional histogram (Left) does not provide the user with the information needed to quickly extract the boundary of the clouds evolution. However, if the user chooses to overlay this histogram with the abstracted attribute of the water vapor (Right), it is easier to extract the precise boundary of the cloud evolution.

The user analyzes the standard deviation of the change in water vapor with respect to the water content distribution. From this analysis, the user selects the discontinuity where the abrupt change in the standard deviation indicates a movement from regions of highly varying water vapor to regions of constant water vapor values. The resultant rendering allows the user to visualize the boundary of the cloud evolution, showing a boundary where there is condensation from vapor to water droplets. The discontinuity would be somewhat near the edges of the visible boundary of the cloud and, as the cloud further evolves, this area may become quite turbulent. This helps show the initial entrainment of dry air into the cloud formation. Using the addition of the water vapor information, the user indicates that they are better able to match their mental model of the simulation to the rendering parameters. Here, the user has a concept of how the water content and water vapor will interact. By adding this information into the histogram visualization and transfer function design phase, the user can feel more comfortable in transfer function exploration and explore more properties of the data simultaneously.

Our final CFD example utilizes the X38 data set based on a tetrahedral finite element viscous calculation computed on geometry configured to emulate the X38 Crew Return Vehicle. The geometry and the simulation were computed at the Engineering Research Center at Mississippi State University by the Simulation and Design Center. This data set represents a single time step in the reentry process into the atmosphere. The simulation was computed on an unstructured grid containing 1,943,483 tetrahedra at a 30 degree angle of attack. however, for ease of testing in collaboration with the CFD researchers to guarantee accuracy, we resampled the data onto a $512 \times 256 \times 128$ regular grid.

Fig. 10 illustrates the application of our abstract attribute space representation when applied to the X38 data set. Here, the user compares the distribution of pressure values around the X38 to the underlying air velocity. In discussing with the domain scientist, we chose to view the standard deviation of the air velocity with respect to pressure. When looking at the plots, the domain scientist was interested in first exploring the high standard deviation of velocity in the low pressure area. This represented the body and the vortex cores (both rendered in blue). Next, the domain

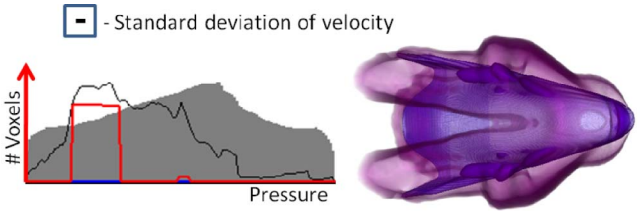

Fig. 10. Exploring the x38 data set with respect to pressure and velocity. The red line in each 1D histogram widget is the user defined opacity.

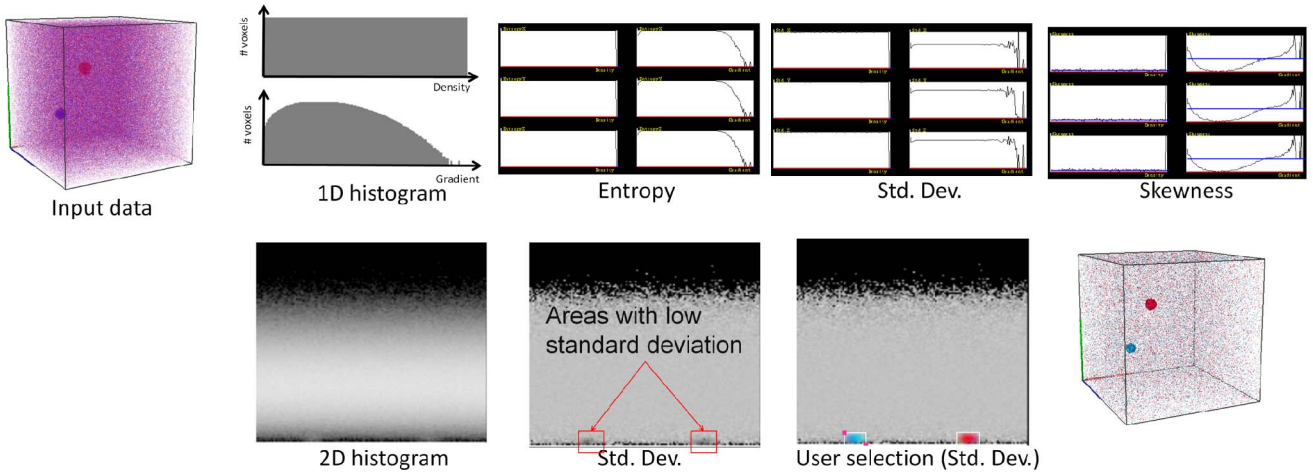

Fig. 11. Comparing the effects of noise on the abstract attribute space. Here, the user is exploring a volumetric data set with a density that approximates a uniform distribution; however, two small spheres are embedded in this distribution. As expected, the results for entropy, standard deviation and skewness match that of a uniform random distribution. However, in the 2D standard deviation abstraction, areas of low standard deviation value become visible indicating areas of interest.

expert also wanted to explore the sharp standard deviation peak in velocity which appears almost as a discontinuity. By interactively selecting these two regions, the scientist can visualize the bow shock, the vortex cores, and the secondary shocks.

While such properties could have been found while exploring the pressure histogram alone, the domain scientist indicated that they like the ability to overlay secondary attributes on the data. The derived properties allowed them to visualize the interaction between pressure and temperature. By seeing these properties matched together, the scientist is able to relate the transfer function design to the physical interaction of properties and found this to be a natural means of analysis.

5.3 Abstracting Attributes in Noisy Data

The final analysis we performed was to explore the effect that noisy data would have on our abstracted attribute derivations. For this, we created a $64 \times 64 \times 64$ cube volumetric data set. The data set contained two small spheres; however, the voxels were distributed within the data set such that the overall histogram distribution of the volume density would be a uniform random distribution. The synthetic data set is shown in Fig. 11.

Fig. 11 explores the derived entropy, standard deviation, and skewness measures of the x, y, and z spatial attributes of our synthetic data set. As expected, the resultant entropy calculations showed a constant high entropy value (the entropy of the uniform random distribution function will be the maximum value entropy can obtain). The standard deviation and skewness also showed properties associated with a uniform random distribution, with the standard deviation being a high constant and the skewness being zero (as the data are symmetrically distributed). Based on these results, the abstraction of the spatial volumetric attributes provides little insight into the data; however, this is as expected given that the underlying data should approximate a uniform random distribution.

Of interest, though, was the 2D histogram showing the density versus density gradient values shown in Fig. 11. When using the standard deviation and the x, y, and z directional components scaled by the view direction, we are able to find small areas in the histogram with a very low standard deviation. From previous examples, areas of low standard deviation represent compact structure within the volume. By selecting these areas, a reasonable rendering of the data can be produced.

Clearly, the application of the abstracted attribute space is sensitive to noise; however, this example was provided to highlight the worst case scenario. As the amount of noise in the data set increases, the amount of information that can be extracted decreases. Assume you have a volumetric feature, with property $f_k = i$, where i would be the histogram bin to which the N voxels making up this feature of interest map to, for example, a velocity, density, etc., that is known to map to a volumetric feature. If there exist M noisy voxels placed randomly in the volume that also have the property $f_k = i$, then this strategy fails if M is greater than $.5N$.

While the results of our abstraction were unsurprising for the uniform random distribution, we also chose to explore noisy CT data in order to evaluate the potential effect of noise. In Fig. 12, we explore a noisy CT foot data set. From our results, we see that the noise found in this data does little to affect the resulting attribute statistics. Moreover, using the spatial skewness close to zero in the 2D histogram (bottom) allows us to avoid choosing noise in the data compared to the traditional transfer function (top).

From these experiments, it is clear that noise will affect the underlying statistical calculations in the abstract attribute space. However, the degree to which this will affect the calculations is based on how the noise is distributed through the entire data set. Our calculations are performed for each bin in the histogram. For any bin in which the distribution is approximately normal, our calculations will return the expected values. However, this is not to say that such a calculation is meaningless. Our attribute space abstraction provides insight into another attribute distribution with respect to value ranges in the primary attribute being analyzed. In this manner, insight

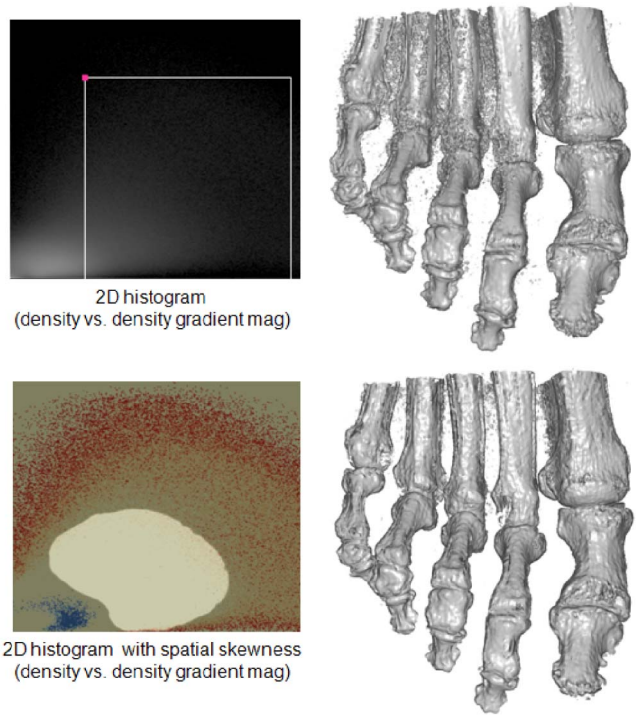

Fig. 12. Comparing explorations of the noisy CT feet data using a traditional 2D histogram widget and the spatial skewness abstracted 2D histogram widget. Here, the user has used a box transfer function on the traditional 2D transfer function (Top), whereas the user has brushed the zero skewness to avoid the noise in the data (Bottom).

can be gleaned from the data as shown in the previous sections.

6 Conclusions and Future Work

Traditionally, the appropriate selection of attributes in multidimensional transfer functions is a difficult task, often requiring the user to have an underlying knowledge of the data set under exploration. By providing users with enhanced information about other attributes of their data in an abstracted attribute space (e.g., density, value versus value gradient magnitude) we are able to enhance the exploration, allowing users to better discover attributes within their data set. Users are able to quickly visualize and explore relationships within a given attribute space, enhancing their knowledge about interactions between the attribute space variables.

Our interactions with domain experts showed that these users tended to favor the mean and standard deviation plots as they were more comfortable with those metrics. Domain experts indicated that they liked the overlay of the abstracted attribute space, and that the added plot enabled them to think about transfer function design as more than a selection of value ranges, but also as a selection of variable interaction ranges. Experiences with the various data sets indicates that entropy was the least used statistical measure for exploration. Skeweness and standard deviation were useful for showing boundary areas and changes in data ranges, while the mean value was useful for direct comparison between two attributes. Often, the mean value calculation was used by domain experts in comparing velocity and pressure, water content and water vapor, etc. Future work will focus on deriving other information metrics including interaction information and cross entropy for measuring attribute complexity. Furthermore, we plan to utilize abstracted attribute space measures for novel volume rendering parameters in order to reduce the burden of transfer function design on the user.

Acknowledgments

This work has been supported by the US Department of Homeland Security's VACCINE Center under Award Number 2009-ST-061-CI0001 and the US National Science Foundation (NSF) under Grants 0328984 and 0121288. Yun Jang has been supported by the Swiss National Science Foundation under grant 200021_124642.

References

[1] T. He, L. Hong, A. Kaufman, and H. Pfister, "Generation of Transfer Functions with Stochastic Search Techniques," *Proc. IEEE Conf. Visualization,* pp. 227-234, 1996.

[2] J. Marks, B. Andalman, P.A. Beardsley, W. Freeman, S. Gibson, J. Hodgins, T. Kang, B. Mirtich, H. Pfister, W. Ruml, K. Ryall, J. Seims, and S. Shieber, "Design Galleries: A General Approach to Setting Parameters for Computer Graphics and Animation," *Proc. ACM SIGGRAPH Conf. Computer Graphics and Interactive Techniques,* pp. 389-400, 1997.

[3] J. Kniss, G. Kindlmann, and C. Hansen, "Interactive Volume Rendering Using Multi-Dimensional Transfer Functions and Direct Manipulation Widgets," *Proc. IEEE Conf. Visualization,* pp. 255-262, 2001.

[4] D.C. Banks and B.A. Singer, "Vortex Tubes in Turbulent Flows: Identification, Representation, Reconstruction," *Proc. IEEE Conf. Visualization (VIS '94),* pp. 132-139, 1994.

[5] K.-L. Ma, J. Van Rosendale, and W. Vermeer, "3D Shock Wave Visualization on Unstructured Grids," *Proc. Symp. vol. Visualization,* pp. 87-95, 1996.

[6] G. Kindlmann and J.W. Durkin, "Semi-Automatic Generation of Transfer Functions for Direct Volume Rendering," *Proc. IEEE Symp. Vol. Visualization,* pp. 79-86, 1998.

[7] M. Levoy, "Display of Surfaces from Volume Data," *IEEE Computer Graphics and Applications,* vol. CGA-8, no. 3, pp. 29-37, May 1988.

[8] C.L. Bajaj, V. Pascucci, and D.R. Schikore, "The Contour Spectrum," *Proc. IEEE Conf. Visualization,* pp. 167-173, 1997.

[9] G. Kindlmann, R. Whitaker, T. Tasdizen, and T. Möller, "Curvature-Based Transfer Functions for Direct Volume Rendering: Methods and Applications," *Proc. IEEE Conf. Visualization,* pp. 513-520, 2003.

[10] F.-Y. Tzeng, E.B. Lum, and K.-L. Ma, "A Novel Interface for Higher-Dimensional Classification of Volume Data," *Proc. IEEE Conf. Visualization,* pp. 505-512, 2003.

[11] S. Potts and T. Möller, "Transfer Functions on a Logarithmic Scale for Volume Rendering," *Proc. Graphics Interface,* pp. 57-63, 2004.

[12] C. Lundström, P. Ljung, and A. Ynnerman, "Multi-Dimensional Transfer Function Design Using Sorted Histograms," *Proc. Eurographics/IEEE VGTC Workshop Vol. Graphics,* pp. 1-8, July 2006.

[13] C. Lundström, P. Ljung, and A. Ynnerman, "Local Histograms for Design of Transfer Functions in Direct Volume Rendering," *IEEE Trans. Visualization and Computer Graphics,* vol. 12, no. 6, pp. 1570-1579, Nov./Dec. 2006.

[14] C. Lundström, A. Ynnerman, P. Ljung, A. Persson, and H. Knutsson, "The Alpha-Histogram: Using Spatial Coherence to Enhance Histograms and Transfer Function Design," *Proc. Eurographics/IEEE-VGTC Symp. Visualization,* pp. 227-234, May 2006.

[15] C. Correa and K.-L. Ma, "Size-Based Transfer Functions: A New Volume Exploration Technique," *IEEE Trans. Visualization and Computer Graphics,* vol. 14, no. 6, pp. 1380-1387, Oct. 2008.

[16] C. Correa and K.-L. Ma, "Visibility-Driven Transfer Functions," *Proc. IEEE-VGTC Pacific Visualization Symp.,* Apr. 2009.

[17] R. Maciejewski, I. Woo, W. Chen, and D.S. Ebert, "Structuring Feature Space: A Non-Parametric Method for Volumetric Transfer Function Generation," *IEEE Trans. Visualization and Computer Graphics,* vol. 15, no. 6, pp. 1473-1480, Nov./Dec. 2009.

[18] S. Bruckner and T. Möller, "Isosurface Similarity Maps," *Computer Graphics Forum,* vol. 29, no. 3, pp. 773-782, 2010.
[19] A. Shamir, "Feature-Space Analysis of Unstructured Meshes," *Proc. IEEE Conf. Visualization,* pp. 185-192, 2003.
[20] S. Roettger, M. Bauer, and M. Stamminger, "Spatialized Transfer Functions," *Proc. Eurographics/IEEE-VGTC Symp. Visualization,* pp. 271-278, 2005.
[21] C. Henze, "Feature Detection in Linked Derived Spaces," *Proc. Conf. Visualization (VIS '98),* pp. 87-94, 1998.
[22] J. Woodring and H.-W. Shen, "Multi-Variate, Time Varying, and Comparative Visualization with Contextual Cues," *IEEE Trans. Visualization and Computer Graphics,* vol. 12, no. 5, pp. 909-916, Sept./Oct. 2006.
[23] H. Akiba and K.-L. Ma, "A Tri-Space Visualization Interface for Analyzing Time-Varying Multivariate Volume Data," *Proc. Eurographics/IEEE VGTC Symp. Visualization,* pp. 115-122, May 2007.
[24] H. Akiba, K.-L. Ma, J.H. Chen, and E.R. Hawkes, "Visualizing Multivariate Volume Data from Turbulent Combustion Simulations," *Computing in Science and Eng.,* vol. 9, no. 2, pp. 76-83, 2007.
[25] C. Muelder and K.-L. Ma, "Interactive Feature Extraction and Tracking by Utilizing Region Coherency," *Proc. IEEE Pacific Visualization Symp.,* pp. 17-24, Apr. 2009.
[26] Z. Fang, T. Möller, G. Hamarneh, and A. Celler, "Visualization and Exploration of Time-Varying Medical Image Data Sets," *Proc. Graphics Interface (GI '07),* pp. 281-288, 2007.
[27] H. Jänicke, A. Wiebel, G. Scheuermann, and W. Kollmann, "Multifield Visualization Using Local Statistical Complexity," *IEEE Trans. Visualization and Computer Graphics,* vol. 13, no. 6, pp. 1384-1391, Nov./Dec. 2007.
[28] M. Haidacher, S. Bruckner, A. Kanitsar, and M.E. Gröller, "Information-Based Transfer Functions for Multimodal Visualization," *Proc. Visual Computing for Biology and Medicine,* pp. 101-108, Oct. 2008.
[29] *Dynamic Graphics for Statistics,* Statistics/Probability Series, W.S. Cleveland and M.E. McGill, eds. Wadsworth & Brooks/Cole, 1998.
[30] *The Visual Display of Quantitative Information,* E.R. Tufte, ed. Graphics Press, 1993.
[31] C. Stolte, D. Tang, and P. Hanrahan, "Polaris: A System for Query, Analysis, and Visualization of Multidimensional Relational Databases," *IEEE Trans. Visualization and Computer Graphics,* vol. 8, no. 1, pp. 52-65, Jan.-Mar. 2002.
[32] D.F. Swayne, D.T. Lang, A. Buja, and D. Cook, "GGobi: Evolving from XGobi into an Extensible Framework for Interactive Data Visualization," *Computational Statistics and Data Analysis,* vol. 43, no. 4, pp. 423-444, 2003.
[33] M.O. Ward, "XmdvTool: Integrating Multiple Methods for Visualizing Multivariate Data," *Proc. IEEE Conf. Visualization (VIS '94),* pp. 326-333, 1994.
[34] N. Elmqvist, P. Dragicevic, and J.-D. Fekete, "Rolling the Dice: Multidimensional Visual Exploration Using Scatterplot Matrix Navigation," *IEEE Trans. Visualization and Computer Graphics,* vol. 14, pp. 1141-1148, Nov./Dec. 2008.
[35] C. Wang, H. Yu, and K.-L. Ma, "Importance-Driven Time-Varying Data Visualization," *IEEE Trans. Visualization and Computer Graphics,* vol. 14, no. 6, pp. 1547-1554, Nov./Dec. 2008.
[36] J. Kehrer, P. Filzmoser, and H. Hauser, "Brushing Moments in Interactive Visual Analysis," *Computer Graphics Forum,* vol. 29, no. 3, pp. 813-822, 2010.
[37] M. Haidacher, D. Patel, S. Bruckner, A. Kanitsar, and M.E. Gröller, "Volume Visualization Based on Statistical Transfer-Function Spaces," *Proc. IEEE Pacific Visualization Symp. '10,* pp. 17-24, 2010.
[38] S. Bachthaler and D. Weiskopf, "Continuous Scatterplots," *IEEE Trans. Visualization and Computer Graphics,* vol. 14, no. 6, pp. 1428-1435, Nov./Dec. 2008.
[39] S. Bachthaler and D. Weiskopf, "Efficient and Adpative Rendering of 2-D Continuous Scatterplots," *Computer Graphics Forum,* vol. 28, no. 3, pp. 743-750, 2009.
[40] H. Carr, B. Duffy, and B. Denby, "On Histogram and Isosurface Statistics," *IEEE Trans. Visualization and Computer Graphics,* vol. 12, no. 5, pp. 1259-1265, Sept./Oct. 2006.
[41] C. Scheidegger, J. Schreiner, B. Duffy, H. Carr, and C. Silva, "Revisiting Histograms and Isosurface Statistics," *IEEE Trans. Visualization and Computer Graphics,* vol. 14, no. 6, pp. 1659-1666, Nov./Dec. 2008.
[42] D. Patel, M. Haidacher, J.-P. Balabanian, and M.E. Gröller, "Moment Curves," *Proc. IEEE Pacific Visualization Symp. '09,* pp. 201-208, Apr. 2009.
[43] C.S. Co, A. Friedman, D.P. Grote, J.-L. Vay, E.W. Bethel, and K.I. Joy, "Interactive Methods for Exploring Particle Simulation," *Proc. Eurographics/IEEE-VGTC Symp. Visualization '05,* pp. 279-286, 2005.
[44] D. Silver and X. Wang, "Tracking and Visualizing Turbulent 3D Features," *IEEE Trans. Visualization and Computer Graphics,* vol. 3, no. 2, pp. 129-141, Apr.-June 1997.
[45] J. Woodring, C. Wang, and H.-W. Shen, "High Dimensional Direct Rendering of Time-Varying Volumetric Data," *Proc. IEEE 14th Visualization (VIS '03),* p. 55, 2003.
[46] N.A. Svakhine, Y. Jang, D.S. Ebert, and K.P. Gaither, "Illustration and Photography Inspired Visualization of Flows and Volumes," *Proc. IEEE Conf. Visualization,* pp. 687-694, 2005.

Ross Maciejewski received the PhD degree in electrical and computer engineering from Purdue University in December, 2009. He is currently an assistant professor at Arizona State University in the School of Computing, Informatics & Decision Systems Engineering. Prior to this, he served as a visiting assistant professor at Purdue University and worked at the Department of Homeland Security Center of Excellence for Command Control and Interoperability in the Visual Analytics for Command, Control, and Interoperability Environments (VACCINE) group. His research interests are geovisualization, visual analytics and nonphotorealistic rendering. He is a member of the IEEE and the IEEE Computer Society.

Yun Jang received the bachelor's degree in electrical engineering from Seoul National University, South Korea, in 2000, the master's and doctoral degrees in electrical and computer engineering from Purdue University in 2002 and 2007, respectively. He is an assistant professor of computer engineering at Sejong University, Seoul, South Korea. He was a postdoctoral researcher at CSCS and ETH Zurich, Switzerland from 2007-2011. His research interests include interactive visualization, volume rendering, and data representations with functions.

Insoo Woo received the BS degree in computer engineering in 1998 from Dong-A University in South Korea and working toward the PhD degree in the School of Electrical and Computer Engineering at Purdue University. He is a research assistant in Purdue University Rendering and Perception Lab. He was employed as a software engineer during 1997 to 2006. His research interest is GPU-aided Techniques for Computer Graphics and Visualization.

Heike Jänicke received the MS degree (Diplom) in computer science with a special focus on medical computer science in 2006 from Leipzig University. For her research of information-theoretic methods in visualization, she was awarded the PhD degree in 2009 from the same university. During 2009 and 2010, she worked as a postdoctoral researcher at Swansea University. Since March 2010, she is working as a junior professor for computer graphics and visualization at Heidelberg University, Germany. Her research interests include data analysis methods from statistics and information theory, visualization of unsteady, multivariate data with applications in biology, medicine, astronomy, and climate research. She is a member of the IEEE.

Kelly P. Gaither received the bachelor's and master's degrees in computer science from Texas A&M University in 1988, and 1992, respectively, and the doctoral degree in computational engineering from Mississippi State University in May, 2000. While obtaining the PhD degree, she worked full time at the Simulation and Design Center in the National Science Foundation Engineering Research Center as the leader of the visualization group. She is the director of Data & Information Analysis at the Texas Advanced Computing Center (TACC) and leads the scientific visualization, data management & collections, and data mining & statistics programs at TACC while conducting research in scientific visualization and data analysis. She, a research scientist, also serves as the area director for visualization in the National Science Foundation funded TeraGrid project. She has a number of refereed publications in fields ranging from Computational Mechanics to Supercomputing Applications to Scientific Visualization. She has given a number of invited talks. Over the past 10 years, she has actively participated in the IEEE Visualization conference, and served as the IEEE Visualization conference general chair in 2004. She is currently serving on the IEEE Visualization and Graphics Technical Committee. She is a member of the IEEE and the IEEE Computer Society.

David S. Ebert received the PhD degree in computer science from Ohio State University. He is a professor in the School of Electrical and Computer Engineering at Purdue University, a University Faculty scholar, director of the Purdue University Rendering and Perceptualization Lab, and director of the Purdue University Regional Visualization and Analytics Center. His research interests include novel visualization techniques, visual analytics, volume rendering, information visualization, perceptually based visualization, illustrative visualization, and procedural abstraction of complex, massive data. He is a fellow of the IEEE and the IEEE Computer Society, and a member of the IEEE Computer Society's Publications Board.